ANNALI DI GEOFISICA, VOL. 42, N. 1, February 1999

The October 9, 1996 earthquake in Cyprus: seismological, macroseismic and strong motion data

Ioannis Kalogeras ([1]), **George Stavrakakis** ([1]) **and Kyriakos Solomi** ([2])
([1]) *National Observatory of Athens, Geodynamic Institute, Athens, Greece*
([2]) *Ministry of Agriculture and Natural Resources, Geological Survey Department, Nicosia, Cyprus*

Abstract
On October 9, 1996, an earthquake of magnitude 6.8 occurred in the sea area SW of Cyprus, Eastern Mediterranean. This earthquake, which caused damage mostly in the area of Paphos and Limassol, triggered an accelerograph installed at Yermasoyia dam, north of Limassol. The Geodynamic Institute of the National Observatory of Athens in cooperation with the Geological Survey of Cyprus deployed five digital accelerographs in order to record large aftershocks. Although the aftershock activity lasted over four months and included a large number of earthquakes with magnitudes 4.5 and greater, only the largest aftershock of January 13, 1997, having a magnitude of 5.9, triggered two of these five accelerographs. Moreover another digital accelerograph, operated by the Water Development Department of Cyprus, was triggered and this record was also taken into account in this study. The first Cyprean strong motion records obtained to date, gave us the opportunity to compare the results from their analysis to the already proposed attenuation relationships from other areas of the world with a similar seismotectonic regime. Although a general fitting to the attenuation curves for subduction events and strike-slip/reverse fault events was found, the calculated peak ground accelerations were found to be lower than others. Unfortunately, due to the lack of data from previous Cyprean earthquakes, it was not possible to conclude to precise attenuation relationships for the area.

Key words *strong motion – attenuation – subduction zone – strike-slip – reverse fault – Cyprus*

1. Introduction - seismotectonics

Cyprus lies on the southern part of the collision boundary between the African and Eurasian plates. This arcuate zone of shortening, the so-called Cyprean arc, extends from the Gulf of Antalia in the west and the Gulf of Iskenderum in the east. In the west the Cyprean arc meets the Hellenic arc under Southern Asia Minor, in an area where subcrustal and intermediate depth earthquakes occurred.

Although the Hellenic arc is extensively studied, the adjacent Cyprean arc is not well defined and understood and this is attributed to its lower seismicity. The seismicity of the Cyprean arc according to Ambraseys and Adams (1993) is much less than that of Greece and Turkey and is comparable only with that of Northern Italy or the Western Mediterranean.

Most studies in the Eastern Mediterranean conclude that the Cyprean arc is a plate boundary. There is very little agreement, however, about the geometry and hence of relative motions in the vicinity of this plate boundary. Figure 1 shows the active tectonics of the area (Robertson *et al.*, 1991).

Mailing address: Dr. Ioannis Kalogeras, Geodynamic Institute, National Observatory of Athens, P.O. Box 20048, GR11810 Athens, Greece; e-mail: i.kalog@egelados. gein. noa.gr

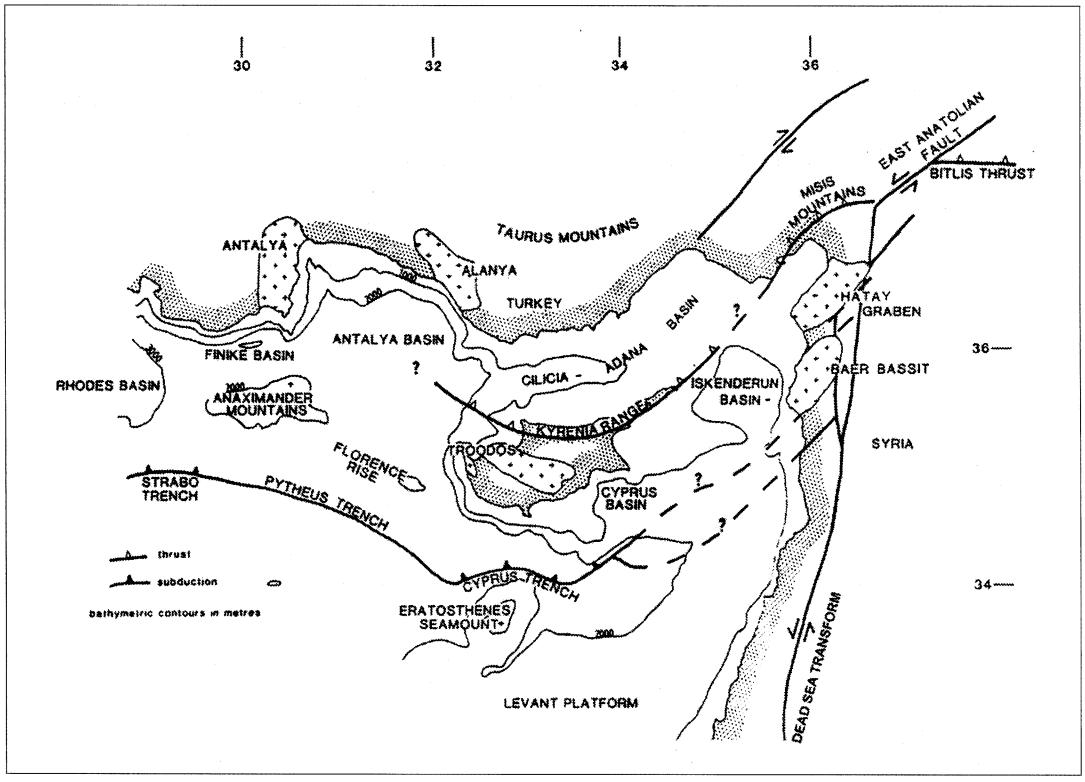

Fig. 1. Map showing the active tectonics of Cyprus and adjacent area (from Robertson *et al.*, 1991).

Dewey and Sengor (1979) and Sengor (1979) suggest that the Cyprean arc forms a continuous plate boundary with the Hellenic arc and that this plate boundary is a zone of convergence west of Cyprus. LePichon and Angelier (1979) suggested that the Cyprean arc is a broad zone of thrusting rather than a distinct plate boundary, and that it is not continuous with the Hellenic arc.

Rotstein and Kafka (1982) suggest that simple subduction along the Cyprean arc is consistent with the dipping seismic zones and the source mechanism solutions in the Eastern Mediterranean. The subduction zone is at present south of the Anaximander mountains and Florence rise which are proposed to be continental fragments. Moreover they believe that thrusting seems to be the dominant mechanism in the vicinity of the Cyprean arc.

Focal plane solutions indicate a Benioff zone off SW and W Cyprus (Pytheus trench), dipping northeast but further east off Southern Cyprus the slab is not well defined and strike slip may dominate (Rotstein and Ben-Avraham, 1985; Kempler and Ben-Avraham, 1987). Earthquakes at subcrustal depths down to about 100 km beneath the north-western part of the arc suggest that subduction is taking place in the Antalian Basin (Jackson and McKenzie, 1984). However, for the rest of the arc the situation is not clear, because the seismological data to the south-east of the Antalian Basin are too few and too unreliable to establish a documented opinion.

Makris (1981) using refraction seismic data, determined that the Mediterranean crust near Cyprus is of oceanic type, which is consistent with the simple subduction of the oceanic litho-

sphere of the African plate beneath the Turkish plate. Nevertheless, Makris *et al.* (1983) found that the island appears to be underlain by continental crust, which may relate to the Eratosthenes Seamount, or some other microcontinent unit (Clube and Robertson, 1986).

Robertson *et al.* (1991) defined a subduction trench south of Cyprus based on bathymetric and seismic data, which curves around the north margin of the Eratosthenes Seamount, broadens and shallows eastwards.

On the other hand, and specifically, for the southwestern part of Cyprus, several models have been proposed to explain strike-slip tectonics in terms of an anti-clockwise rotation of a microplate. The most extensive palaeomagnetic studies (Clube *et al.*, 1985; Clube and Robertson, 1986; Abrahamsen and Schonharting, 1987) indicated an anti-clockwise rotation of 60° in Campanian – early Maastrichtian times. Rotation of microplates is known to take place in a variety of tectonic settings, like those of forearc oceanic areas (Fuller *et al.*, 1983), triple junctions along oceanic rises (Searle *et al.*, 1989), areas adjacent to strike-slip fault zones (Kissel *et al.*, 1987).

2. Seismicity in Southwestern Cyprus

It becomes apparent from the map of fig. 2 that the spatial distribution of the epicentres in and near Cyprus defines areas of lower seismic-

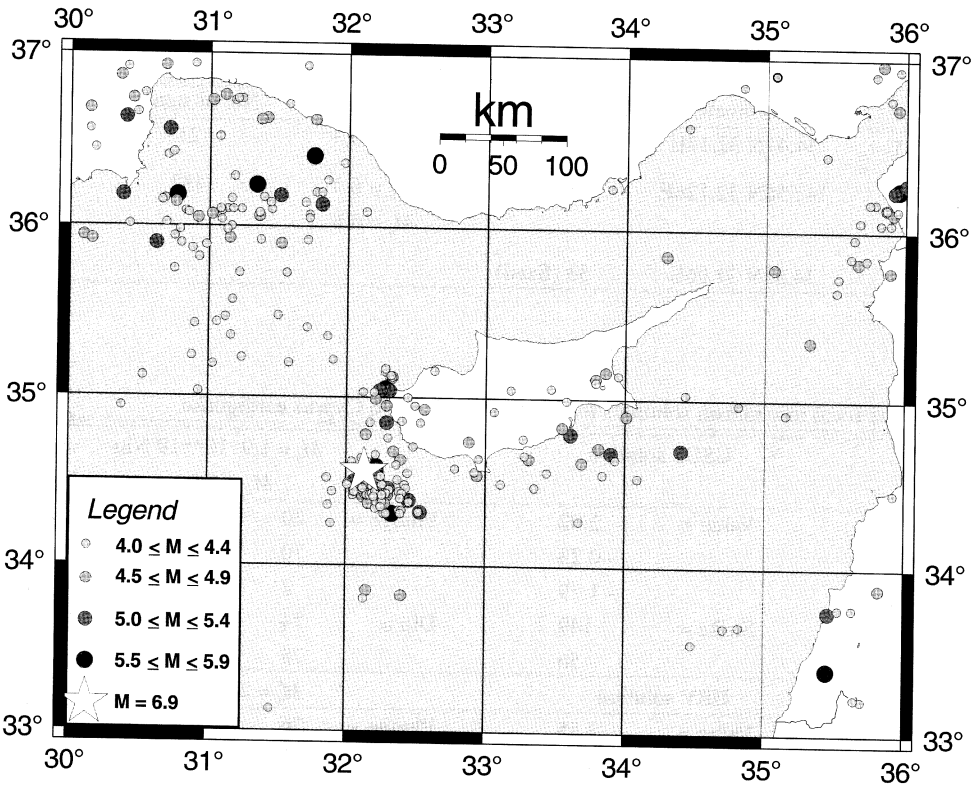

Fig. 2. Seismicity map of Cyprus and adjacent areas. The earthquakes plotted occurred between 1900 and 1997 and their magnitudes were 4.0 and greater. The data are taken from USGS databases and the map was been created using Generic Mapping Tools (Wessel and Smith, 1995)

ity, for example between Antalia Gulf and Cyprus, northwest of the island, and between Iskenderum bay and Cyprus, northeast of the island. On the other hand, the epicentres southwest and south-southeast of the island are more dense.

Southwestern Cyprus has suffered a lot of earthquakes in the past. The most interesting earthquakes during the present century were those of May 9, 1930; September 10, 1953; September 12, 1963; January 12, 1976; July 30, 1986 and February 23, 1995. Towns like Paphos and Limassol and villages like Emba, Stroumbi, Peyia, Axylou, Kithasi, Phasoula, Episkopi were damaged or even totally destroyed by the above earthquakes. The event of 1953, which is characterized as a double event with magnitudes 6.0 and 6.1 (Ambraseys and Adams, 1993), caused the death of 40 people, the injury of 400 people, and the total destruction of Stroumbi, Axylou, Kithasi, Lapithiou and Phasoula. Generally, the strongest of these earthquakes were felt throughout the whole island as well as in Lebanon, Israel, Turkey and Egypt.

These are described in detail by Ambraseys and Adams (1993).

3. Seismic parameters of the aftershock sequence

The seismic parameters of the earthquake of 9 October 1996 were calculated by the Geodynamic Institute using the first arrival of stations of Israel, Cyprus and of the network of the Institute. A second trial using the closest to the

Table I. Seismic parameters of the October 9, 1996 Cyprus earthquake.

Origin time	Coordinates	Depth (km)	Magnitudes	No. of stations	References
13:10:52.1	34.41N 32.12E	25	$M_L = 6.3$	21	GI
13:10:52.1	34.556N 32.126E	33 (fixed)	$M_b = 6.4$ $M_S = 6.8$	482	USGS
13:11:05.1	34.82N 31.96E	33 (fixed)			HRV

Table II. The focal mechanism solutions for the October 9, 1996 Cyprus earthquake.

	USGS solution			$M_0 = 1.9*10**19$ Nm $M_w = 6.8$		
T	Value =	2.02	Plunge =	20	Azimuth =	12
N		– 0.23		70		199
P		– 1.79		2		103
NP1	Strike =	149	Dip =	74	Slip =	13
NP2		56		78		164
	HRV solution			$M_0 = 2.1*10**19$ Nm		
T	Value =	2.55	Plunge =	26	Azimuth =	3
N		– 0.83		63		167
P		– 1.72		7		270
NP1	Strike =	43	Dip =	67	Slip =	165
NP2		139		77		– 24

epicentre stations gave roughly the same results. The calculation of the magnitude was based on the readings of one instrument, that of the Athens Wood – Anderson, and although the epicentral distance was quite large – 800 km – the magnitude found was not far from those calculated by other institutes. Tables I and II summarize the results of the seismic parameter estimation by Geodynamic Institute (GI), USGS and Harvard (HRV).

The main shock was followed by a large number of aftershocks during the following 4 months. Many of them were of magnitude 4.5, some of them of magnitude 5.0. On 13th January 1997 at 10:19 the strongest aftershock occurred with a local magnitude of 5.6.

The parameters of this aftershock calculated by the Geodynamic Institute using data obtained from its stations as well as the Cyprean and the Israel stations are listed in tables III and IV along with the solutions of USGS and Harvard.

The map of fig. 3 marks the location of the two shocks and their focal mechanisms, as well as the epicentre and the focal mechanism of the event of February 23, 1995 are shown.

4. Observed damage

Although the earthquake was quite strong, no significant ground changes were caused. No rocks fell and no landslide, ground subsidence or ground liquefaction were reported, except a case of detachment of a large mass of rocks near Pissouri and a crack of the asphalt of a road in Paphos area, Southwestern Cyprus.

Table III. Seismic parameters of the January 13, 1997 aftershock.

Origin time	Coordinates	Depth (km)	Magnitudes	No. of stations	References
10:19:25.7	34.27N 32.37E	20	$M_L = 5.6$	21	GI
10:19:26.11	34.305N 32.326E	33 (fixed)	$M_b = 5.3$	372	USGS
			$M_S = 5.4$		
10:19:30.7	34.06N 32.25E	33 (fixed)			HRV

Table IV. The focal mechanism solutions for the January 13, 1997 aftershock.

	USGS solution			$M_0 = 3.3*10**17$ Nm $M_w = 5.6$		
T	Value =	3.33	Plunge =	33	Azimuth =	344
N		– 0.05		57		169
P		– 3.28		2		76
NP1	Strike =	125	Dip =	66	Slip =	2.3
NP2		25		69		154
	HRV solution			$M_0 = 4.3*10**17$ Nm		
T	Value =	4.58	Plunge =	19	Azimuth =	147
N		– 0.47		70		341
P		– 4.10		4		238
NP1	Strike =	284	Dip =	73	Slip =	11
NP2		191		80		163

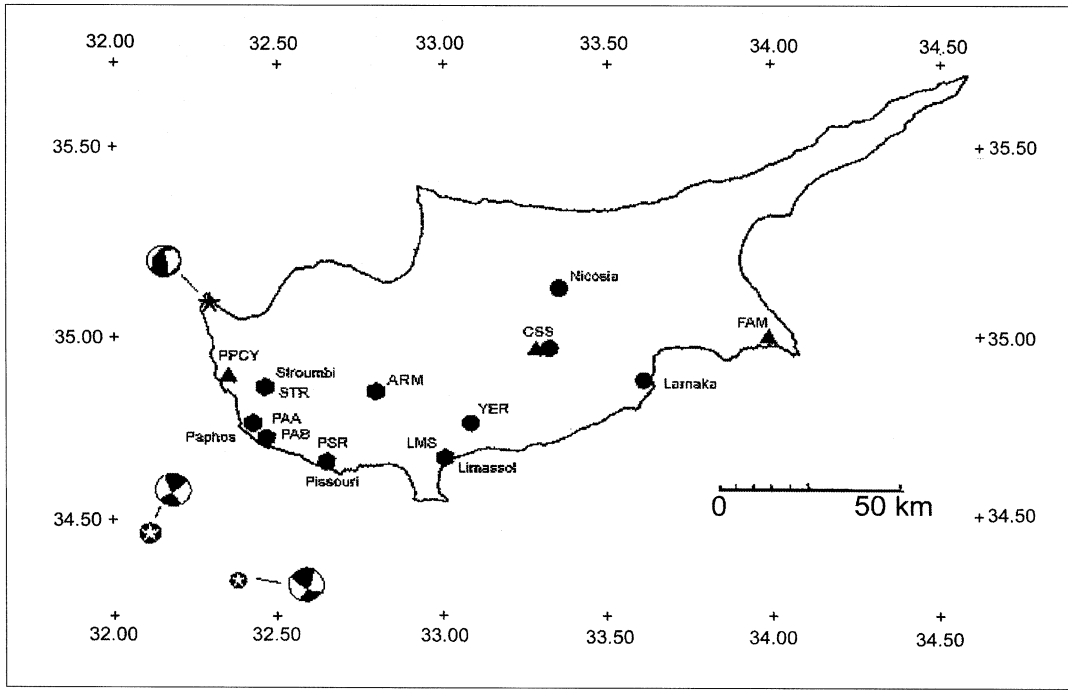

Fig. 3. Map showing the location of the instruments, the location of the epicentres and the respective focal mechanisms. Solid triangles and circles show the sites of the seismographs and accelerographs of the Geological Survey of Cyprus, respectively. Hexagons show the sites of the digital accelerographs of Geodynamic Institute and of Water Development Department of Cyprus (ARM). Big star in circle is the epicentre of the October 9, 1996 main shock, while small star in circle is its aftershock of January 13, 1997. Their focal mechanisms are also shown. For comparison, the epicentre (denoted by solid star) of the February 23, 1995 earthquake and its focal mechanism are shown in the figure.

The buildings that were checked by the engineers, just after the main shock, could be classified as neoclassic brick-built 2-storey, concrete-reinforced 2-storey with pilotis, apartment buildings of 3 to 5 storeys, churches, mainly stone-built and schools.

Table V summarizes the observed damage classified according to the districts of Cyprus. The reported data were taken from the Earthquake Rehabilitation Service of Cyprus and they were evaluated by the Geological Survey of Cyprus. The total cost of damage repairs reached the amount of 20 million US dollars.

It is apparent that the severly damaged buildings are distributed in Paphos district, although villages in the area, such as Arodes, Latsi, Peyia, which suffered from the 1995 earthquake, were not damaged by this earthquake.

Generally, the observed damage was not considerable, compared to the magnitude of the earthquake. Although in some cases collapses were observed (like the collapse of the bell tower in Stroumbi, a village NNE from Paphos) the mean intensity for the entire town or village does not exceed the VIII of the Modified Mercalli (MM) scale.

In conclusion, the damage may be attributed more to the bad construction or to the fact that the damaged buildings suffered from previous earthquakes. Slight damage was observed even in Paralimni, Southeastern Cyprus. The map of fig. 4 shows schematically the distribution of the

Table V. Summary of the observed damage classified according to the districts of Cyprus.

District	Total building damage		Heavy damage		Medium damage		Light damage	
	Number	%	Number	%	Number	%	Number	%
Paphos	3500	25	500	3.6	1300	9.3	1700	12.1
Limassol	5000	10	500	1	1500	3	3000	6
Larnaka	400	2	10	0.05	90	0.45	300	1.5
Nicosia	700	1	50	0.07	250	0.35	400	0.57
Famagusta	1	0.01	–	–	1	0.01	–	–

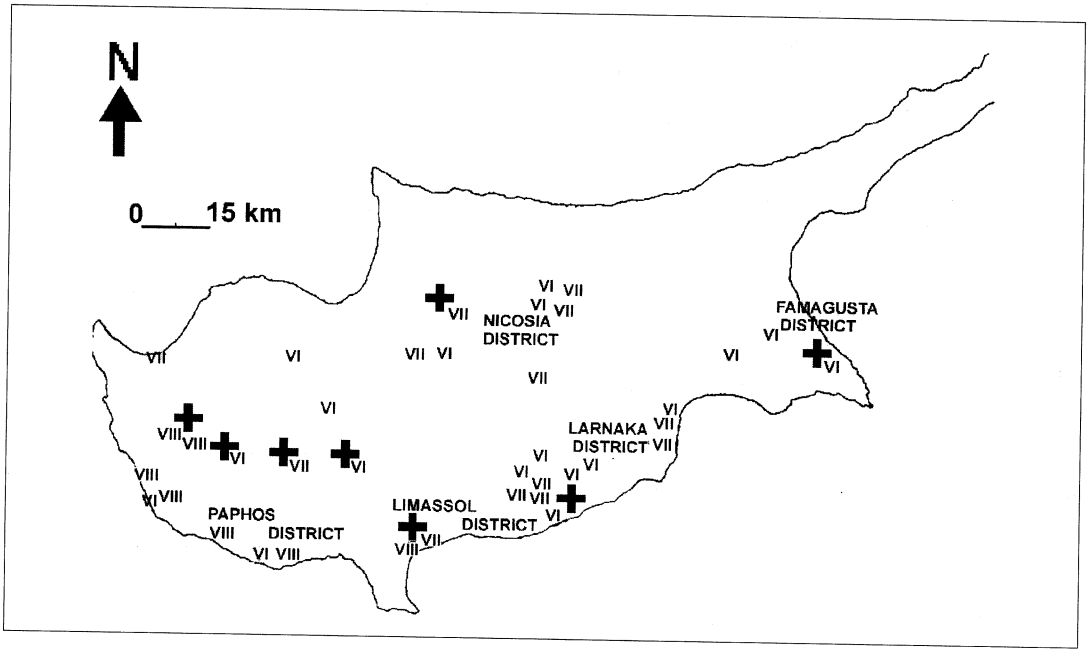

Fig. 4. Map showing the sites of the observed damage. The roman numbers refer to the Modified Mercalli (MM) intensity scale. Crosses show sites of damaged bell towers of churches. The damage is generally not considerable and randomly distributed throughout the island.

observed damage. The roman numbers refer to the Modified Mercalli scale. Crosses show the sites of damage on churches. No observations were made in the northern and north-eastern part of the island because it is under Turkish occupation.

No further damage was caused by aftershocks, even the strongest of them (13th January 1997).

5. Instrumentation and strong motion data analysis

The Geological Survey of Cyprus operates three analog accelerographs, SMA-1 type, which are installed at Yermasoya dam, at Mathiati seismological station and in Nicosia. The triggering level of these instruments has been set to 0.01 *g*.

The Water Development Department of Cyprus also operates some accelerographs for monitoring the behaviour of the dams.

The Geodynamic Institute, shortly after the main shock, installed five digital accelerographs, A-800 type. For the deployment of this small network the epicentre location, as well as the observed damage, the geological structure and the urban planning were taken into account. The accelerographs were installed in Limassol, at Pissouri, in the city centre of Paphos, on the coast of Paphos and at Stroumbi. The orientation of the longitudinal component of the instruments was the same (N-S) and the triggering level of these accelerographs was set quite low – at 0.002 g – because it was considered that the small damage was due to absorption of the seismic energy. This was proved true, as only two of these five instruments were triggered by the largest aftershock on 13th January 1997. No other aftershock triggered any of the accelerographs. This largest aftershock also triggered a digital accelerograph operated by the Water Development Department of Cyprus and installed at Arminou Dam.

Table VI shows information about the instruments whose recordings were used in this study.

The strong motion records were analyzed by the method developed in the Geodynamic Institute based on the standard procedure of the CALTECH Institute. We use the same procedure even for the digital records after we convert them to a format acceptable by vol2 of the software. The detailed procedure is described in Stavrakakis *et al.* (1993). Table VII summarizes the results.

Table VI. Information about instruments and sites

Location	Coordinates		Building	Geology	Comments
	φ°N	λ°E			
Yermasoya Dam	34.73	33.08	One-story R/F.C. building	Marly chalk	Warehouse
Limassol	34.67	33.04	One-story prefabricated building	Sands, clays, gravels	Department of Public Works
Pissouri	34.65	32.72	One-story R/F.C. building	Sandstones, marly limestone	Hotel Columbia
Paphos	34.69	32.44	Basement of 4-story R/F.C. building	Calcareous sandstone	Hotel Phaethon
Paphos	34.77	32.42	Basement of 2-story R/F.C. building	Calcareous sandstone	Police HQ
Stroumbi	34.88	32.48	Basement of 2-story R/F.C. building	Sands, marls, limestone	Community Office
Arminou Dam	34.87	32.73	One story R/F.C. building	River deposits over pillow lavas	Water Supplies Company

Table VII. Summary of the peak corrected acceleration of the strong motion records.

Code	Earthquake		Distance (km)	Peak corrected acceleration (cm/s^2)		
				Longitudinal	Vertical	Transverse
YER1	9/10/1996	13:11	95	27.2	33.1	43.4
LMS1	13/1/1999	10:19	76	12.8	4.98	13.5
PSR1	13/1/1999	10:19	53	9.57	7.1	11.1
ARM1	13/1/1999	10:19	74	12.09	4.68	15.48

6. Discussion and conclusions

The largest aftershock triggered only three digital accelerographs. Although the rest of the instruments installed by the Geodynamic Institute were deployed at equal or even shorter epicentral distances, such as 47 km for Paphos beach, 56 km for Paphos centre and 68 km for Stroumbi, and they were set to equal triggerring level (0.002 g), they were not triggered. This observation on its own could be attributed to the local conditions of the site of installation. However, the random distribution and the relatively low grade of the damage observed, lead to the examination of the tectonic regime and the focal mechanism as the causes of those observations. Different tectonic environments, like stable continental regions, subduction zones or shallow earthquakes in active tectonic regions, give rise to different ground motion attenuation relationships.

The parameters that must be clearly defined in order to estimate ground motions are: earthquake magnitude, type of faulting, distance and local site conditions. Moment magnitude is the preferred magnitude measure because it is directly related to the seismic moment of the earthquake. Style of faulting is also considered in most recent attenuation relationships because reverse and thrust earthquakes tend to generate larger PGA and high-frequency SA than strike-slip and normal earthquakes. Regardless of tectonic regime, rupture directivity also affects ground motion attenuation relationships.

Most subduction zone events are recorded at large distances because the events tend to be deep or offshore, with the exception of the 1985 Michoacan earthquake for which the records came from distances of 13 km. So, there is a difficulty for the extrapolation of the attenuation models at distances less than 30 km (Abrahamson and Shedlock, 1997).

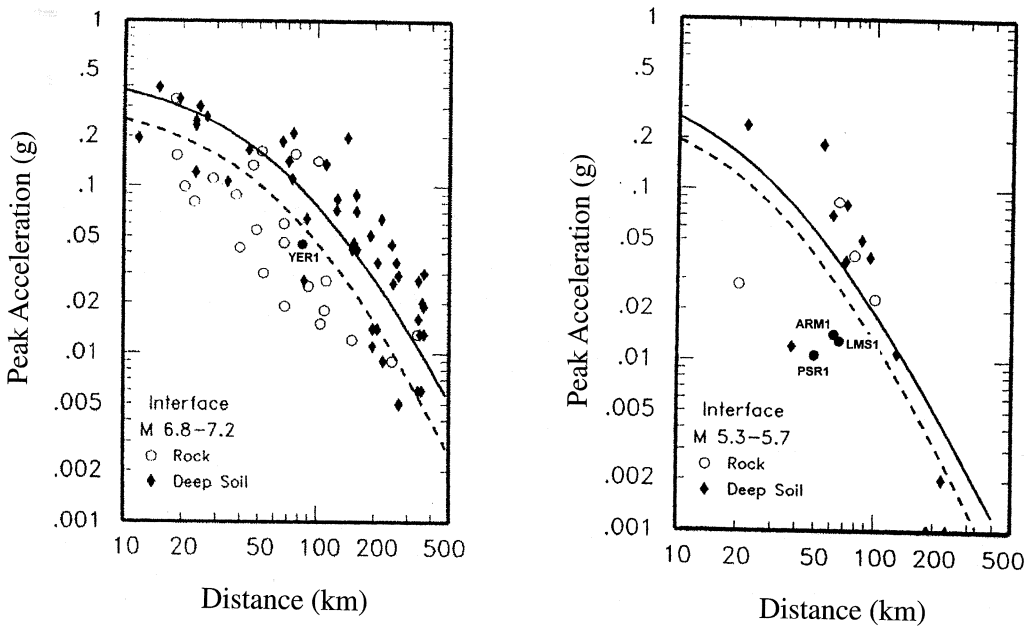

Fig. 5. Predicted peak ground acceleration values using interface events with moment magnitudes between 6.8 and 7.2 (left) and between 5.3 and 5.7 (right) from Youngs *et al.* (1997). Dashed lines fit the rock site data and the solid line the deep soil site data. The calculated value of the main shock (YER1) fits the rock site data quite well, while the calculated values for the aftershock (ARM1, PSR1 and LMS1) are found to be lower than other data. Due to the wide scattering, it is difficult to say for the calculated values which line they fit better.

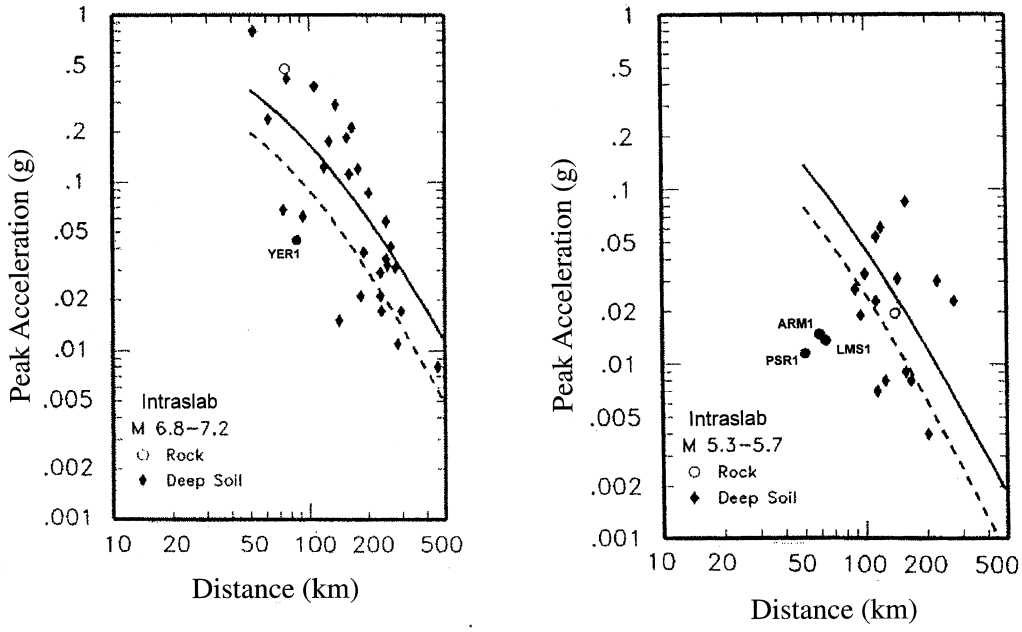

Fig. 6. The same as fig. 5, but for intraslab earthquakes after Youngs *et al.* (1997). It is again apparent that the calculated values are lower than other especially for the aftershock of January 13, 1997. The fitting to the curves for rock sites as well as for deep soil sites seems to be worse compared to the fitting of the interface events.

Youngs *et al.* (1997) considered two types of earthquakes in subduction zones, interface and intraslab earthquakes. The interface earthquakes are shallow thrust events that occur at the interface between the subducting and overriding plates. Intraslab earthquakes occur within the subducting oceanic plate and are typically high-angle, normal faulting events responding to downdip tension in the subducting plate. They illustrated that peak ground motions from subduction zone earthquakes attenuate more slowly than those from shallow crustal earthquakes in tectonically active regions and intraslab earthquakes produce larger peak ground motions than interface earthquakes for the same magnitude and distance.

Although these two types of earthquakes are distinguished from shallow crustal earthquakes that occur within the upper 20-25 km of the continental crust, some investigators believe that the ground motions from interface earthquakes and shallow crustal earthquakes are similar, at least in Japan. The differentiation between interface and intraslab events was done on the basis of the faulting mechanism or on the basis of the focal depth. Tichelaar and Ruff (1993) indicate that interface earthquakes worldwide nearly all occur at depths shallower than 50 km.

In order to examine the values of peak acceleration recorded in conjunction with the seismotectonic regime, we use the diagrams of Youngs *et al.* (1997) after we reevaluated the parameters involved, namely the peak ground acceleration, the distance and the magnitude. Peak ground acceleration is represented by the geometric mean of the two horizontal components. Youngs *et al.* (1997) use the closest distance to rupture surface, r_{rup}, so assuming that the strike of the rupture surface is 45° we found that we have to decrease the epicentral distance a little in order to have the r_{rup}. Admittedly, the differences were too small to interfere with the

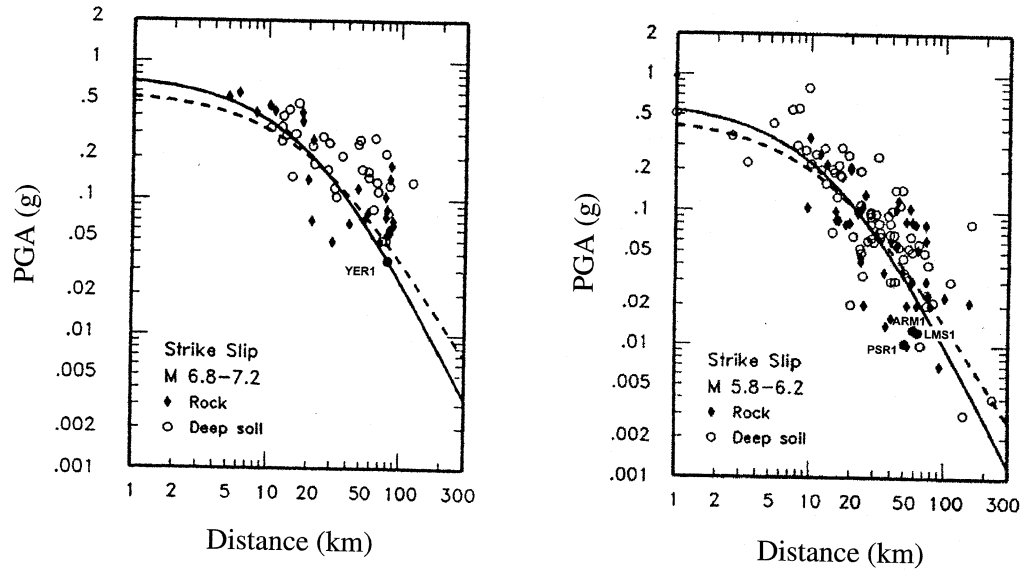

Fig. 7. Predicted peak ground acceleration values for normal and strike slip crustal earthquakes from Sadigh *et al.* (1997). The values calculated in our study have been placed in the graphs, left for the mainshock and right for the aftershock. The solid line is for rock site events and the dashed line for the deep soil events. A fitting to the rock site curves is apparent, but the values are lower than to other calculated values.

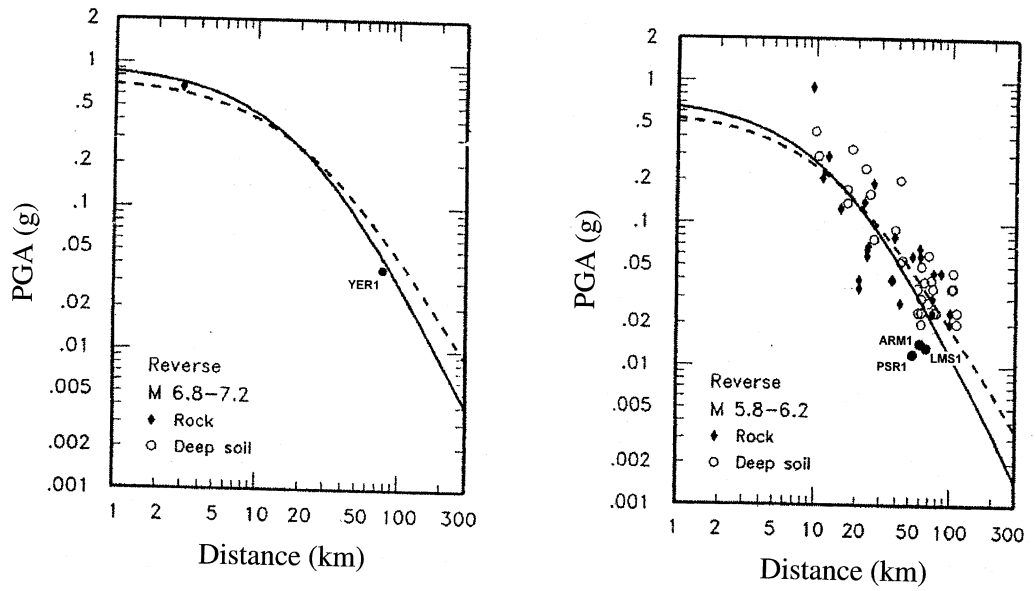

Fig. 8. The same as fig. 7, but for reverse faulting earthquakes (Sadigh *et al.*, 1997). Again, there is a good fitting to the rock site curves (although there is not enough data for large earthquakes), but the calculated values of our study are lower than others.

conclusions. We found for the main shock with an epicentral distance 95 km and a depth 25 km, r_{rup} = 85 km, and for the aftershock with epicentral distances 53, 74 and 76 km and depth 20 km, r_{rup} = 50, 63 and 65 km respectively.

As for the magnitude, the moment magnitude is used, according to Hanks and Kanamori relation (1979). We used the seismic moment reported by Harvard and we found M = 6.8 for the main shock and M = 5.7 for the aftershock.

We then placed the peak acceleration values estimated in this study in the Youngs *et al.* (1997) graphs. Figure 5 shows the predicted peak ground acceleration for interface events and for magnitudes M = 6.8-7.2 (left) and M = 5.3-5.7 (right). The solid line represents the deep soil site data and the dashed line the rock site data. The values of YER1 in the left graph of the figure and of ARM1, LMS1 and PSR1 in the right graph fit quite well the rock site curves. Figure 6 shows the predicted peak ground acceleration for intraslab events and for magnitudes M = 6.8-7.2 (left) and M = 5.3-5.7 (right). Again the solid line is for deep soil site data and the dashed line is for rock site data. It is rather unlikely to say that from only one value from a rock site the respective curve is representative. Nevertheless, the three calculated values ARM1, LMS1 and PSR1 (right) are apparently lower than the predicted ones for these distances, while the YER1 value (left) is closer to the curve.

Additionally, we compared our results with the curves for predicted peak ground acceleration values from crustal events. Sadigh *et al.* (1997) presented attenuation relationships for shallow crustal earthquakes determined from strong motion data recorded mainly in California. In this work two data sets were considered, that with earthquakes of normal and strike-slip faulting (with rake angle > 45°, fig. 7) and that with earthquakes of reverse faulting (with rake angle < 45°, fig. 8). The placing of the normal faulting earthquakes in the same set with the strike-slip events was done due to the small number of this kind of earthquakes in most data sets and due to the conclusion that, statistically, the normal faulting events generate the same level of ground motion as strike-slip events (Abrahamson and Shedlock, 1997).

Although these are the only available strong motion records from Cyprus, a general agreement of the calculated values with the predicted ones is obvious, with a tendency for them to be on the lower boundary of the attenuation curves. In cases like this, when few data exist, the most precise possible calculation of the focal depth and of the focal mechanism could support the final selection of the attenuation curve which should be used.

In the case of the October 9, 1996 and the January 13, 1997 earthquakes, the focal mechanism solutions showed a reverse/strike-slip fault, while the long epicentral distances (> 50 km) and the shallow focal depths (< 30 km) led to subduction interface events.

Acknowledgements

This work was carried out within the frame of the bilateral research and technology cooperation between Greece and Cyprus (1996-1997) which is financed by the General Secretariat of Research and Technology (Greece) and the Central Programming Committee (Cyprus). The authors are grateful to Dr. G. Milana and Dr. M. Mucciarelli for their constructive comments.

REFERENCES

ABRAHAMSEN, N. and G. SCHONHARTING (1987): Palaeomagnetic timing of the rotation and translation of Cyprus, *Earth Planet. Sci. Lett.*, **81**, 409-418.

ABRAHAMSON, N.A. and K.M. SHEDLOCK (1997): Overview, *Seismol. Res. Lett.*, **68** (1), 9-23.

AMBRASEYS, N.N. and R.D. ADAMS (1993): Seismicity of the Cyprus region, *Terra Nova*, **5** (1), 85-94.

CLUBE, T.M.M and A.H.F. ROBERTSON (1986): The palaeorotation of the Troodos microplate, Cyprus, in the Late Mesozoic – Early Cenozoic plate tectonic framework of the Eastern Mediterranean, *Surv. Geophys.*, **8**, 375-437.

CLUBE, T.M.M., K.M. CREER and A.H.F. ROBERTSON (1985): The palaeorotation of the Troodos microplate, Cyprus, *Nature*, **317**, 522-525.

DEWEY, J.F. and A.M.C. SENGOR (1979): Aegean and surrounding areas: complex multi-plate and continuum tectonics in a convergent zone, *Geol. Soc. Am. Bull.*, **90**, 84-92.

FULLER, M., R. MCCABE, I.S. WILLIAMS, J. ALMASCO, R.Y. ENCINA and S. ZANORIA (1983). Palaeomagnetism in Luzon, in *The Tectonic and Geologic Evolution of Southeast Asian Seas and Islands, Part 2*, edited

by D.E. HAYES, *Part 2, Am. Geophys. Union, Geophys. Monograph*, **27**, 79-94.

HANKS, T.C. and H. KANAMORI (1979): A moment magnitude scale, *J. Geophys. Res.*, **84**, 2348-2350.

JACKSON, J. and D. MCKENZIE (1984): Active tectonics of the Alpine-Himalayan Belt between Western Turkey and Pakistan, *R. Astron. Soc. Geophys. J.*, **77**, 185-264.

KEMPLER, D. and Z. BEN-AVRAHAM (1987): The tectonic evolution of the Cyprean arc, *Ann. Tectonicae*, **1**, 58-71.

KISSEL, C., C. LAJ, A.M.C. ENGOR and A. POISSON (1987): Palaeomagnetic evidence for rotation in opposite senses of adjacent blocks in Northeastern Aegean and Western Anatolia, *Geophys. Res. Lett.*, **14**, 907-910.

LEPICHON, X. and J. ANGELIER (1979): The Hellenic arc and trench system: a key to the neotectonic evolution of the Eastern Mediterranean, *Tectonophysics*, **60**, 1-42.

MAKRIS, J. (1981): Deep structure of the Eastern Mediterranean deduced from refraction seismic data (abstract), *Eos, Trans. Am. Geophys. Un.*, **62** (17), 6247.

MAKRIS, J., Z. BEN-AVRAHAM, A. BEHLE, A. GINZBURG, P. GIESE, A. STEINMETZ, S. ELEFTHERIOU and B. WHITMARSH (1983): Deep seismic soundings between Cyprus and Israel and their interpretation, *R. Astron. Soc. Geophys. J.*, **75**, 5750-5791.

ROBERTSON, A.H.F., S. EATON, E.J. FOLLOWS and J.E. MCCALLUM (1991): The role of local tectonics *versus* global sea-level change in the Neogene evolution of the Cyprus active margin, *Spec. Publ. Int. Ass. Sediment.*, **12**, 331-369.

ROTSTEIN, Y. and Z. BEN-AVRAHAM (1985): Accretionary processes at subduction zones in the Eastern Mediterranean, *Tectonophysics*, **112**, 551-561.

ROTSTEIN, Y. and A.L. KAFKA (1982): Seismotectonics of the southern boundary of Anatolia, Eastern Mediterranean region: subduction, collision and arc jumping, *J. Geophys. Res.*, **87** (B9), 7694-7706.

SADIGH, K., C.-J. CHANG, J.A. EGAN, F. MAKDISI and R.R. YOUNGS (1997): Attenuation relationships for shallow crustal earthquakes based on California strong motion data, *Seismol. Res. Lett.*, **68** (1), 180-189.

SEARLE, R.C., R.I. RUSBY, J. ENGEIN, R.N. HEY, J. JUKIN, P.M. HUNTER, T.P. LEBAS, H.-J. HOFFMAN and R. LIVERMORE (1989): Comprehensive sonar imaging of the eastern microplate, *Nature*, **341**, 701-705.

SENGOR, A.M.C. (1979): The North Anatolian transform fault: its age, offset and tectonic significance, *J. Geol. Soc. London*, **136**, 269-282.

STAVRAKAKIS, G., I. KALOGERAS and J. DRAKOPOULOS (1993): Preliminary analysis of greek accelerograms recorded at stations of NOA's network. Time period: 1973-1990, in *Proceedings 2nd Congress Hellenic Geophys. Union, Florina, Greece, 5-7 May*, 175-191.

TICHELAAR, B.W. and L.J. RUFF (1993): Depth of seismic coupling along subduction zones, *J. Geophys. Res.*, **98**, 2017-2037.

YOUNG, R.R, S.-J. CHIOU, W.J. SILVA and J.R. HUMPHREY, (1997): Strong ground motion attenuation relationships for subduction zone earthquakes, *Seismol. Res. Lett.*, **68** (1), 58-189.

WESSEL, P. and W.H.F. SMITH (1995): The Generic Mapping Tool (GMT), Version 3, Technical Reference and Cookbook, pp. 77.

(received September 25, 1998;
accepted January 28, 1999)